

Behaviour and design of demountable steel column-column connections

Dongxu Li ^{*1}, Brian Uy ^{1,2a}, Vipul Patel ^{3b} and Farhad Aslani ^{1,4c}

¹ Centre for Infrastructure Engineering and Safety, School of Civil and Environmental Engineering, The University of New South Wales, Sydney, NSW 2052, Australia

² School of Civil Engineering, The University of Sydney, Sydney, NSW 2006, Australia

³ School of Engineering and Mathematical Sciences, College of Science, Health and Engineering, La Trobe University, PO Box 199, Bendigo, VIC 3552, Australia

⁴ School of Civil, Environmental and Mining Engineering, The University of Western Australia, Crawley, WA 6009, Australia

(Received February 04, 2016, Revised June 14, 2016, Accepted October 13, 2016)

Abstract. This paper presents a finite element (FE) model for predicting the behaviour of steel column-column connections under axial compression and tension. A robustness approach is utilised for the design of steel column-column connections. The FE models take into account for the effects of initial geometric imperfections, material nonlinearities and geometric nonlinearities. The accuracy of the FE models is examined by comparing the predicted results with independent experimental results. It is demonstrated that the FE models accurately predict the ultimate axial strengths and load-deflection curves for steel column-column connections. A parametric study is carried out to investigate the effects of slenderness ratio, contact surface imperfection, thickness of cover-plates, end-plate thickness and bolt position. The buckling strengths of steel column-column connections with contact surface imperfections are compared with design strengths obtained from Australian Standards AS4100 (1998) and Eurocode 3 (2005). It is found that the column connections with maximum allowable imperfections satisfy the design requirements. Furthermore, the steel column-column connections analysed in this paper can be dismantled and reused safely under typical service loads which are usually less than 40% of ultimate axial strengths. The results indicate that steel column-column connections can be demounted at 50% of the ultimate axial load which is greater than typical service load.

Keywords: steel columns; column-column connection; robustness design; demountability; finite element analysis

1. Introduction

Recently, many buildings are being demolished due to redevelopment and their inability to meet the needs of new owners and occupants. This early demolition leads to a significant waste of

*Corresponding author, Ph.D. Student, E-mail: d.li@unsw.edu.au

^a Professor, E-mail: b.uy@unsw.edu.au

^b Lecturer, E-mail: v.patel@latrobe.edu.au

^c Senior Lecturer, E-mail: farhad.aslani@uwa.edu.au

natural materials and produces 40% of landfill waste (Green Building Council of Australia 2009). In addition, most of the greenhouse gas (GHG) emissions are attributed to the production and transport of construction materials, such as cement, concrete and steel. To lower these negative influences on the environment, measures such as reducing and reusing construction materials can be carried out. Furthermore, compared with other construction materials, structural steel can be recycled many times without compromising or loss of material properties before being recycled (Winters-Downey 2010). Because of this unique advantage, structural steel buildings can be disassembled into various components and reused under proper guidance. Gorgolewski (2006) and the Swedish Institute of Steel Construction (2005) investigated the structural steel flows and found that the actual reuse of structural steel is only 10-15%. Therefore, there is a large potential market for the reuse of structural steel.

Steel column-column connections are used to join individual columns in steel framed structures (see Fig. 1). The steel columns with length up to three storeys are typically transported to the construction site. Therefore, it is necessary to connect individual steel columns for multi-storey construction. The steel column-column connections are generally designed to transmit the axial compression between the connected columns. Axial tension should be carried by the steel column-column connections when designing for the case of the bottom steel columns removal in accidental damage. The steel column-column connections can be constructed by a welding process but a welded connection cannot be easily disassembled after its useful service life. An alternative is to use bolted connections between the column above and column below, which thereby makes the steel structures demountable.

Most previous researchers on steel column-column connections have been focused on the load carrying capacity and stiffness of column-column connections. Snijder and Hoenderkamp (2008) conducted experiments on pin-ended steel column-column connections under axial compression. Lindner (2008) conducted full scale tests on steel column-column connections. He investigated the effects of imperfections on the load-deformation curves of the steel column-column connections under axial compression. Uy *et al.* (2015) utilised the finite element analysis package ABAQUS to study the behaviour of demountable composite column-column connections under axial tension.

The above literature review demonstrates that most of these studies on steel column-column connections have been devoted to their ultimate structural behaviour, but the studies on demountable steel connections have not been conducted. The concept of demountable connections

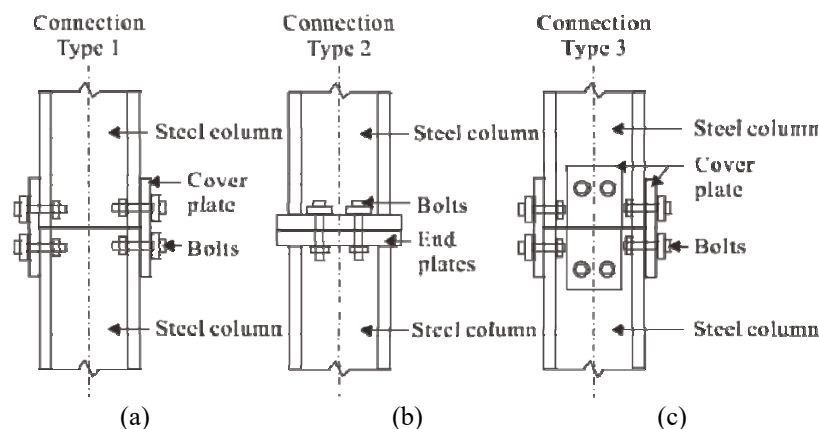


Fig. 1 Typical steel column-column connection types

was first presented by Uy (2014) who suggested that the column-column connections must resist the axial tension when designing for removal of bottom columns in accidental damage. The advantage of the demountable concept was that the steel column and connections could deform elastically, which results in the reuse of steel columns after their useful service life.

As the experiments were conducted up to ultimate axial strengths which induced permanent plastic deformation, further studies are needed for simulating the steel column-columns allowing making demountable. Therefore, extensive FE analysis is conducted herein, which provides an in-depth understanding into the concept of demountable steel column-column connections. The previously tested connections were modified to allow them to be demounted under service loads.

2. Finite element analysis#

2.1 Basic concept

Even though full-scale tests can be used to predict the behaviour of steel column-column connections, they are time consuming and expensive to examine the effects of every parameter on the behaviour of steel column-column connections. It is not adequate to deduce a procedure for the design of steel column-column connections using relatively limited experimental data. Full-scale tests should be utilised to validate a procedure for the design of steel column-column connections instead of deriving the theory. The finite element analysis package ABAQUS (2012) is employed for the nonlinear analysis of demountable steel column-column connections.

2.2 Finite element model

All parts of the test specimens, including steel columns, end plates and bolts were modelled with three-dimensional solid elements. A finite element model is depicted in Fig. 2. The end plates and steel columns were modelled using 8-node linear brick elements with reduced integration (C3D8R). A twenty-node quadratic brick element with reduced integration (C3D20R) was chosen for bolts due to their ability to capture stress concentration more effectively (Mirza and Uy 2011).

In the FE model, the mesh size also played an important role in achieving the accuracy and normally a finer mesh increase the accuracy of the model. In this analysis, a mesh convergence

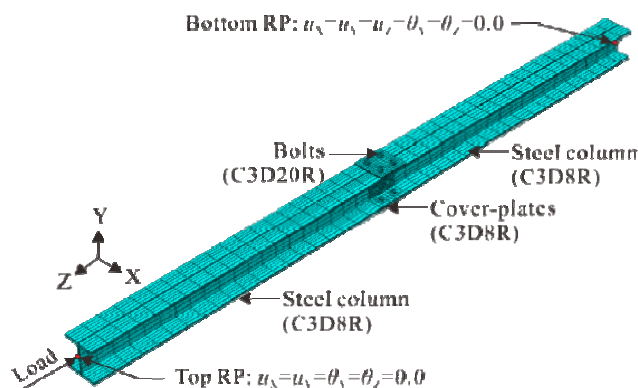


Fig. 2 FE model for steel column-column connection with FE mesh and boundary conditions

study was conducted to provide a rational mesh size, which secures the accuracy whilst reducing the computational time. Based on the sensitivity analysis, the element size for column section is determined to be $L/70$, in which L represents the total length of the column connection (see Fig. 2).

For the cover-plate and the end-plate, the mesh size was taken as $w/20$, where w is the width of cover- or end-plate. $D/3$ was adopted as the mesh size for the bolt and nut, with D representing the bolt diameter. Both ends of the steel column-columns were constrained by the pin-ended boundary conditions. All nodes on the top and bottom surfaces of the connections were tied with centrally located reference point. The axial load, tension or compression, was applied on the top reference point. The pin-ended boundary conditions were assigned to the top and bottom reference points, respectively. The boundary conditions are shown in Fig. 2.

2.3 Interactions between components

Surface-to-surface contact with a Hard Contact Model in the normal direction with no penetration was considered for all contact surfaces. A Coulomb friction model in the tangential direction was assumed with a coefficient of friction. The appropriate value of the coefficient of friction depends on the surface treatment given in Eurocode 3 (2005) and it is taken as 0.25 for cleaned surfaces. This value is also suggested by Lee *et al.* (2010).

The surfaces, which come into contact (see Fig. 3) and are assigned as surface-to-surface contact, are the inner surface of the cover-plates to the outer surface of the steel columns (Contact A), top column to bottom column (Contact B), bolt head to cover-plate and bolt nut to column flange (Contact C), bolt shank to bolt holes (Contact D), as well as the top end-plate to bottom end-plate (Contact E). Apart from the contact interactions, the definition of constraints between column-section and end-plate in connection Type 2 shall be carried out properly. The constraint, Tie, was employed to model all welds. This is because no weld failure was observed in the test specimens (Lindner 2008, Snijder and Hoenderkamp 2008).

2.4 Material properties for structural steel

The material property of the structural steel, which includes column section, cover-plates and high-strength bolts is summarised below:

- (a) Steel grade S235 was used for the steel column sections and cover-plates. Based on the tensile coupon test results (Lindner 2008), this material has an actual minimum yield stress f_{sy} of 254 MPa and an ultimate strength f_u of 360 MPa. Therefore, in the developed FE model, the constitutive behaviour of the steel with actual properties is utilised. In addition, the other material properties specified in ABAQUS include the elastic modulus of steel E_s and Poisson's ratio ν_s , which are taken as 210,000 MPa and 0.3, respectively.
- (b) The behaviour of the structural bolts is normally different from structural steel. This study utilised the full range stress-strain curve based on the test results from Hanus *et al.* (2011).

2.5 Influence of initial geometric imperfections

An eigenvalue buckling simulation of the steel column-column connection is a prerequisite for obtaining an accurate prediction of structural behaviour with initial geometric imperfections (Mago and Hicks 2016). The deflection of all nodes was recorded in the eigenvalue buckling analysis. The deflection of nodes from the eigenvalue buckling analysis serves as the input for the

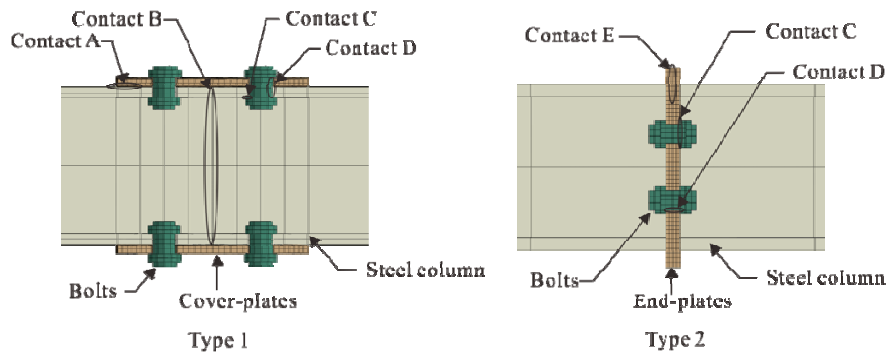


Fig. 3 Interaction details of various components for steel column-column connections

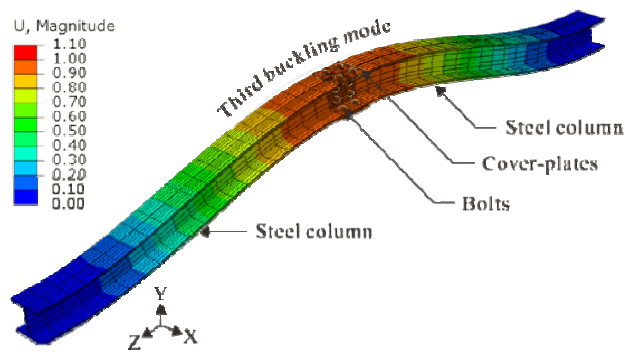


Fig. 4 Buckling mode for slender steel column-column connections

nonlinear static analysis. The finite element mesh is identical in both eigenvalue buckling analysis and nonlinear static simulation. The eigenvalue buckling mode is depicted in Fig. 4. It should also be noted that the column-column connection was forced to buckle about its major axis by adopting the geometric deformation of the third buckling mode. Therefore, the selected buckling mode based on the eigenvalue is not the smallest, which induces buckling about the minor axis. The magnitude of the initial geometric imperfection was assigned by defining an initial deflection at the mid-height of the column-column connection. In this study, the initial geometric imperfection for the slender column was taken as $L/5000$, which was suggested by Hassanein and Kharoob (2014) and An *et al.* (2012).

2.6 Verification of finite element models

2.6.1 Connection type 1

Lindner (2008) conducted 15 tests on short column-column connections with slenderness ratio varying from 18 to 24. The connection is located at the mid-height in the longitudinal direction for the HE 200B (S235) column sections. Table 1 presents the geometric and material properties of two specimens, which were used to validate the FE models. The FE models for Tests 1 and 3 were developed and shown in Fig. 5. In particular, Test 1 is 1300 mm long and the initial surface imperfection was so small that it could be ignored. Test 3 describes the specimen with a total length of 2000 mm. The initial inclination between column sections perpendicular to the X-axis

Table 1 Test results to calibrate FEM with design Type 1

Specimen	Column Section	L (mm)	f_{sy} (MPa)	ψ (°)	ϕ (°)	N_u (kN)	Ref.
Test 1	HE200B	1300	254	0.01	0.04	1930	Lindner (2008)
Test 3	HE200B	2000	254	0.4	0.2	1649	

was ψ (0.4°); while the inclination perpendicular to the Y-axis was ϕ (0.2°), shown in Fig. 6.

Fig. 7 illustrates the comparison between the experimental and finite element results. It can be seen from Fig. 7 that the initial stiffness obtained from the FE model agrees reasonably well with the experimental data. The finite element predictions deviate from the experimental results after achieving the ultimate axial strengths. The deviation in the post-peak behaviour does not affect the accuracy of the model since demountable connections need to be simulated in elastic region.

2.6.2 Connection type 2

Snijder and Hoenderkamp (2008) conducted 18 slender column-column connection tests with slenderness ratio varied between 80 and 210. The column-column connections were made of two end-plates, which were welded to the end of each column section. The connection is located at three-quarter heights in the longitudinal direction for the HE 100A (S235) column sections.

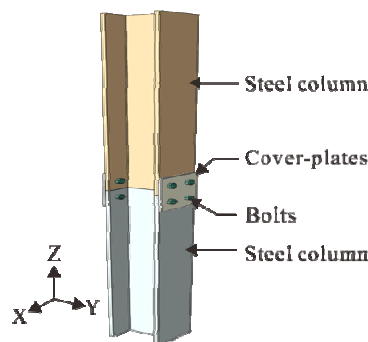


Fig. 5 Configuration of specimens Test 1 and Test 3

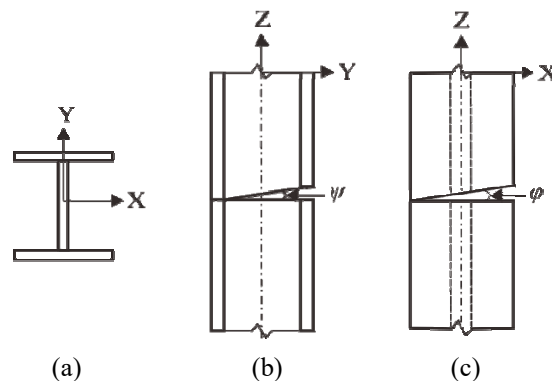


Fig. 6 Initial contact surface imperfections for steel column-column connections

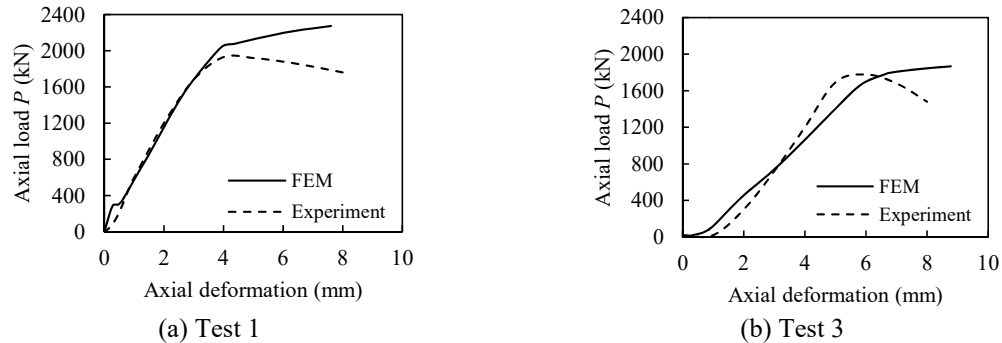


Fig. 7 Comparison between the experimental and FE results for Test 1 and Test 3 (Lindner 2008)

In the finite element models, the column-column connection was pin-supported at both ends. Only deformation along the longitudinal direction and buckling about the strong axis was allowed.

In order to compare the experimental results, transverse deflections at three-quarter height and mid-height were recorded. Furthermore, the initial contact surface imperfections were ignored due to the welding between the column end-section and end-plate.

The finite element models for Specimens 3 and 5 are shown in Fig. 8. It is noted that Specimen 3 has a length of 3390 mm and Specimen 5 is 4530 mm long. Fig. 9 compares the experimental and finite element results in terms of transverse deflection at three-quarter height and mid-height of the column-column connections. It can be observed from Fig. 9 that the finite element results agree well with the experimental results except the three-quarter height, where the connection is located.

Table 2 compares the compressive strength between the experimental and finite element results. It can be seen from Table 2 that the buckling strength obtained from the finite element models (N_{FEM}) is slightly lower than the test results (N_{Test}). The difference between the experimental and finite element analysis may be attributed to the fact that the friction of the testing frame restrained the specimen from buckling about the Y-axis.

Overall, the finite element models developed for the steel column-column connections agree reasonably well with the experimental results. The verified finite element models were utilised for investigating the important parameters on the fundamental behaviour of the steel column-column connections.

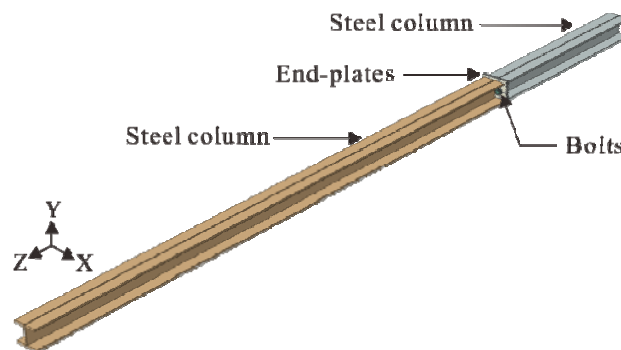


Fig. 8 Configuration of Specimens 3 and 5

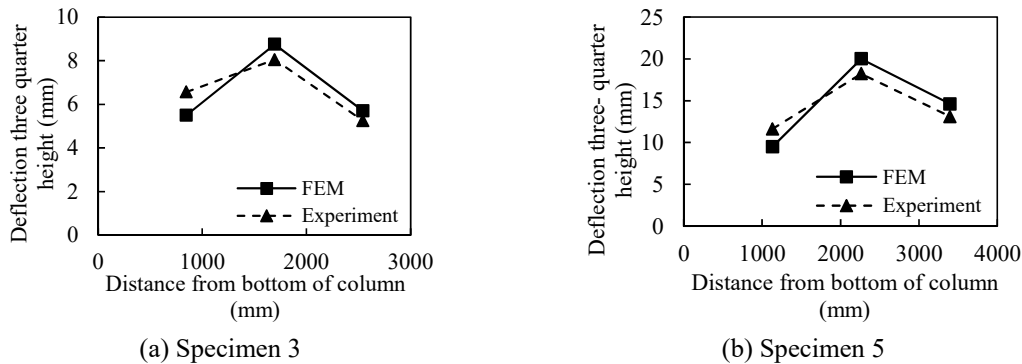


Fig. 9 Comparison of transverse deflections along column-column connection between experimental and FE results for Specimens 3 and 5 (Snijder and Hoenderkamp 2008)

Table 2 Comparison of ultimate strength between experiment and FE results for Specimens 3 and 5

Specimens	Column section	L (mm)	f_{sy} (MPa)	N_{Test} (kN)	N_{FEM} (kN)	N_{FEM}/N_{Test}	Ref.
Specimen 3	HE100A	3390	298	574	521	0.91	Snijder and Hoenderkamp (2008)
Specimen 5	HE100A	4530	298	370	335	0.91	

3. Steel column-column connections under accidental loading

Current practical design codes state that for steel column-column connections with members prepared for full contact bearing, the connection shall be designed to provide for continuity of stiffness and be capable of transmitting 25% of the maximum compressive force. However, there is no detailed guidance for steel column-column connections under axial tension.

As stated in Eurocode 1 (2006), the column-column connection is subjected to axial tension when a bottom column is removed after exhibiting accidental damage. Fig. 10 illustrates the column-column connection in a steel frame. It can be seen from the figure that if the bottom column is removed from the frame after exhibiting damage, the loading pattern of the connection shall be reversed from compressive to tensile. The design equation given in AS1170 (2002) for determining the ultimate tensile strength of a column-column connection is expressed by

$$T_c = \eta \times N_c \quad (1)$$

where N_c represents the ultimate axial strength under axial compression and η reflects the factor which accounts for the accidental damage and it is expressed by

$$\eta = \frac{N_1}{N_o} \quad (2)$$

in which N_o denotes the axial compression before the accidental damage. An empirical equation for determining this axial compression (N_o) of a column without accidental damage is given in AS1170 (2002) as follows

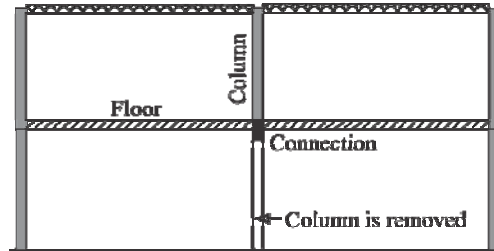


Fig. 10 Schematic steel frame showing the removal of bottom column under accidental damage

$$N_o = 1.2G + 1.5Q \quad (3)$$

in which G represents the dead load in kPa and Q is live load and taken as 3.0 kPa (AS1170, 2002). In Eq. (2), N_1 represents the axial compression after the column exhibits the accidental damage such as in a blast, fire or earthquake. The axial compression (N_1) can be determined by the equation given in AS1170 (2002) and is given by

$$N_1 = G + \psi_1 Q \quad (4)$$

in which ψ_1 represents the factor for live load after the accidental damage. The factor (ψ_1) is taken as 0.3 for cyclic loading and 0.4 for fire (AS1170 2002). As provided by Li *et al.* (2015), the reduction factor (η) given in Eq. (2) is determined as 0.51 and 0.54 for cyclic loading and fire, respectively. It should be noted that the column-column connections are required to resist the tensile load up to approximately half of the ultimate compressive strength of column.

4. Results and discussion

4.1 Comparison of various connection types

This paper presents the finite element models for various steel column-column connection types, which are most commonly used in the construction industry (see Fig. 11). The column-column connections are designed based on practical design codes and robustness design consideration stated in Section 3. In the developed FE models, column section HE 200B was utilised and the total length of the connection was 4270 mm. The geometric details of each model are illustrated in Table 3. The yield strength and ultimate strength of the structural steel utilised in the following FE models was 254 MPa and 360 MPa, respectively. The high-strength bolts utilised for the following FE models are M24 with 10.9 grade.

The behaviour of three different connection types is compared in Fig. 12. It can be seen from Fig. 12(a) that the strength and initial stiffness of these connections under axial compression is almost same, except connection Type 2 with end-plate joints has a slightly higher ultimate axial strength. Fig. 12(b) presents the behaviour of these connections under axial tension; the horizontal line is the tension capacity from robustness design given in Section 3. The figure indicates that all connection types exceed the design tension capacity. It can also be seen that connection Type 2 has the largest tensile strength of 1547 kN and initial stiffness, which is attributed to the use of very thick end-plates (40 mm). This connection type fails with the yielding of bolts and the strength of

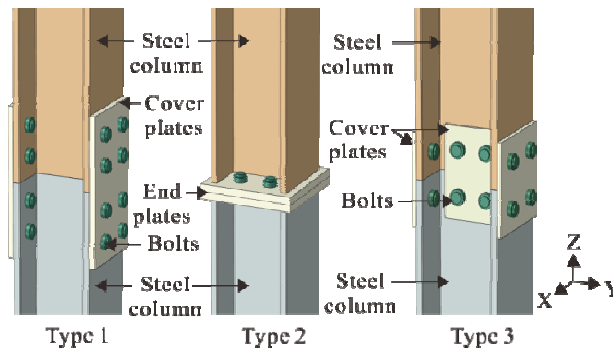


Fig. 11 FE models for various steel column-column connections

Table 3 Details of various column-column connections for numerical study

Specimen type	Cover-plate size on flange (mm)	Cover-plate size on web (mm)	End-plate size (mm)	No. of Bolts	P_{FEM} (kN)	T_{FEM} (kN)
Type 1	340 × 200 × 15	-	-	16	2237	1396
Type 2	-	-	240 × 240 × 40	4	2303	1547
Type 3	200 × 200 × 15	200 × 140 × 8	-	12	2292	1464

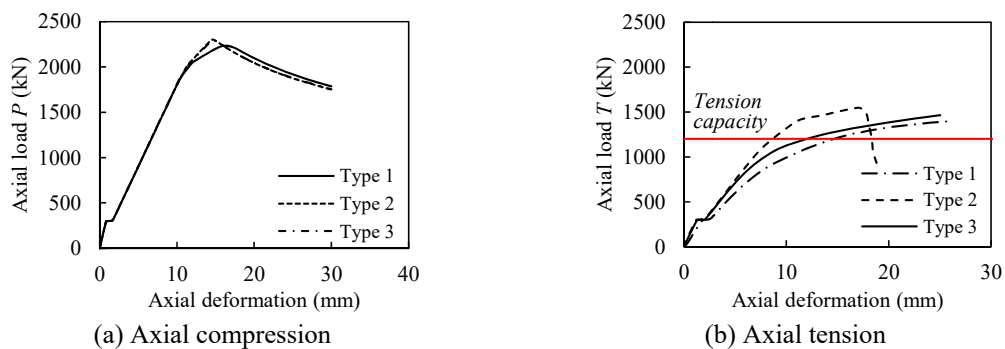


Fig. 12 Load-deformation behaviour of various connection types under axial loading

bolts being fully utilised. However, the use of structural steel in the Type 2 connection is about 2.5 times of the connections Type 1 and 3. Moreover, connection Type 3 achieves a 5% higher tensile strength and stronger initial stiffness than connection Type 1 with 20% less of steel being used. The better performance of connection Type 3 is due to the fact that the high stiffness is secured by utilising cover-plates in both axes for the column-column connection. The parametric study was carried out for investigating the effects of the geometric and material parameters on the fundamental behaviour of the steel column-column connections.

4.2 Parametric study

4.2.1 Effect of slenderness ratio (λ)

The slenderness ratio (λ) is one of the most important factors that influence the behaviour of the

column-column connections. Slenderness ratio (λ) of the specimen was determined by

$$\lambda = \frac{L}{r} \quad (5)$$

where L is the total length of the column-column connection, and r is the radius of gyration of the cross-section of the column, which can be determined as

$$r = \sqrt{\frac{I}{A}} \quad (6)$$

in which I is the second moment of area of the column section and A is the column cross-section area.

Steel column-column connections of Type 1 with total length of 1500 mm, 3000 mm, 5000 mm and 7000 mm were modelled, which have a corresponding slenderness ratio of 18, 35, 58 and 82, respectively. The effect of slenderness ratio (λ) on the axial load-deformation curves for steel column-column connections of Type 1 is illustrated in Fig. 13(a). It can be observed that the initial stiffness and ultimate axial strength decreases as the slenderness ratio increases. The axial load-deformation curves for very slender column-column connections are distinguished by the drop from the pre-peak to the post-peak stages.

The effect of slenderness ratio on axial load-deformation curves for connection Types 2 and 3 is presented in Figs. 13(b) and (c). Generally, the increase of slenderness ratio induces the reduction

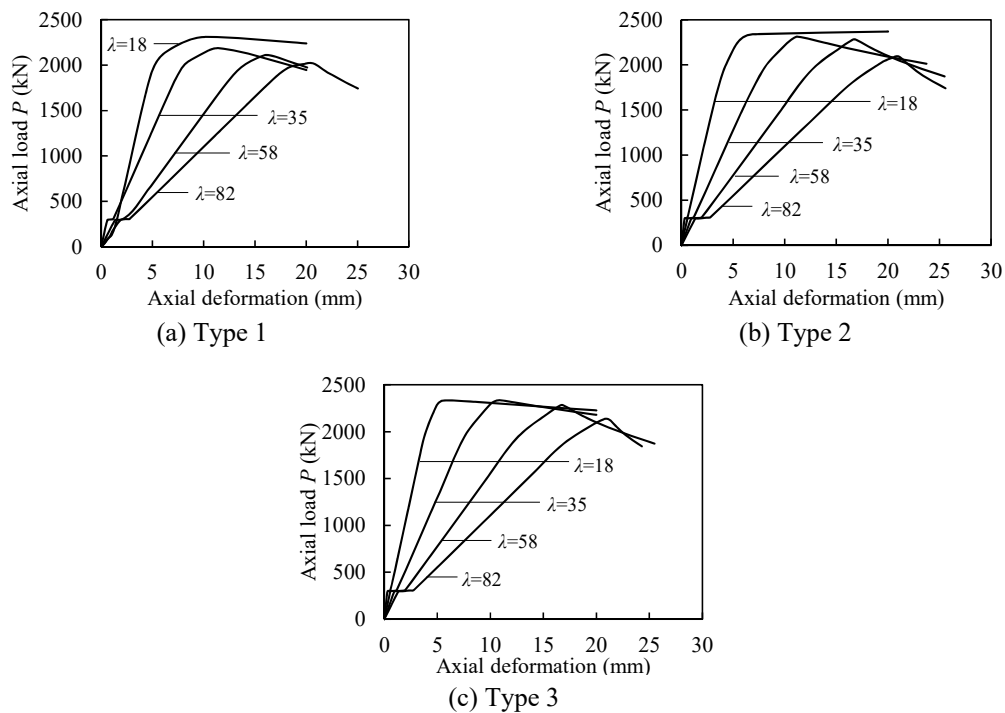


Fig. 13 Effect of slenderness ratio on load-deformation curves for steel column-column connections

of compressive strength and initial stiffness. However, it can be observed from Fig. 13(c) that the ultimate compressive strength of connection Type 3 decreases slightly until the slenderness ratio reaches 58, which is attributed to the higher stiffness of the connection.

4.2.2 Effect of contact surface imperfection (ψ and ϕ)

When cutting the steel I-section columns into two parts, there is a spatial gap between two single parts of the column. These gaps create an initial contact surface imperfection. AS4100 (1998) requires the maximum tolerated inclination of 0.57° for this particular column section (HE200B), which corresponds to a maximum 2 mm gap.

This paper investigates the effects of contact surface imperfection along the X-axis (ψ) and along Y-axis (ϕ) on the load-deformation curves for slender column-column connection Type 1. In the FE model, slender column-column connections utilised HE 200B as column sections and the total length is 4270 mm. It is observed from Fig. 14 that an increase of inclination between the two contact surfaces along both axes decreases the initial stiffness and ultimate compressive strength. It can also be found that the contact surface inclination increases from 0.14° to 0.57° only results in a 40 kN (2%) reduction in ultimate compressive strength. This is because the inclination only induces the buckling of column connections, while compressive strength largely depends on the buckling behaviour of the connection. It can also be concluded from Figs. 14(a) and 14(b) that the inclination along the strong axis leads to a larger reduction in the ultimate axial strength of the connection due to the buckling about the weaker axis.

It can be seen from Fig. 14(c) that the inclination along the strong axis governs the buckling behaviour when the column-column connections are subjected to inclinations along both axes.

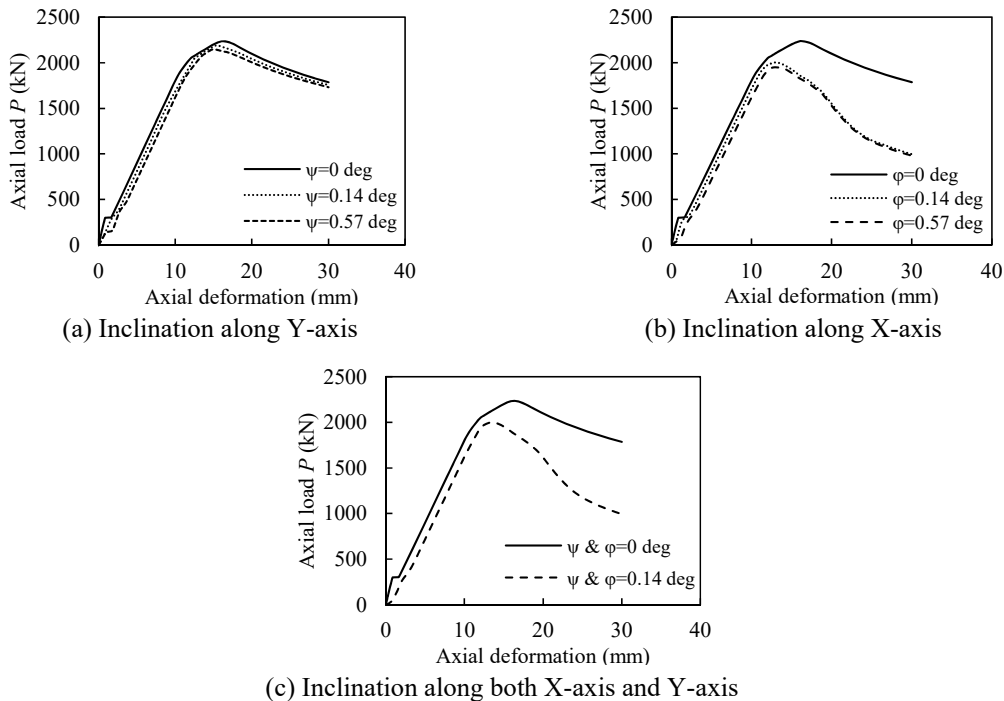


Fig. 14 Effect of contact surface imperfections on load-deformation curves for steel column-column connection of Type 1

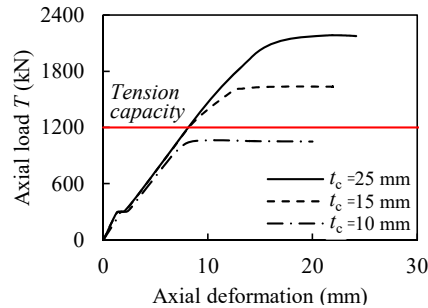


Fig. 15 Effect of cover-plate thickness on the load-deformation curves for column connection of Type 1

This is due to the fact that the buckling about the weaker axis is easier to occur when inclination along both axes exists without lateral bracing being provided in the weaker axis.

Since welding was used between the column section and end-plates for connection Type 2, the effects of contact surface imperfections on the behaviour are ignored. For connection Type 3 with cover-plates in flanges and web, similar results and conclusions can be obtained.

4.2.3 Effect of cover-plate thickness (t_c)

For column-column connections with full contact bearing and subjected to axial compression, cover-plates serve to hold the column sections in position and the thickness of the cover-plate does not influence the axial load-deformation curves of the connection. However, when the connections are subjected to axial tension, the cover-plates transfer the tensile load from the upper column to the bottom through a number of bolts. The effect of cover-plate thickness on the load-deformation curves of connection Type 1 under axial tension is presented in Fig. 15.

It can be observed from Fig. 15 that the ultimate tensile strength increases with an increase in the cover-plate thickness (t_c) and the initial stiffness is not affected significantly. The horizontal line indicates the design tensile strength required by the robustness approach given in Section 3, which is about 50% of the axial compressive strength of the connection. The connection with 15 and 10 mm thick cover-plates leads to the yielding of the cover-plates and the connection with 10 mm thick cover-plates cannot meet the tension capacity required by the robustness approach. On the other hand, the connection with thicker cover-plates (25 mm) ensures the connection fails by column section yielding. However, 25 mm cover-plates not fail by yielding, since the tensile strength of the connection based on robustness design can be satisfied with a 15 mm thick cover-plate.

4.2.4 Effect of end-plate thickness (t_e)

Although steel column-column connections with end-plate joints have been commonly used in the construction industry, it is still difficult to demonstrate that the end-plates meet the requirements in design codes. The common practice for this type of connection is to ensure the plate thickness is large enough or enlarge end-plate size with additional bolts arranged outside the profile of the section. This paper investigates the effect of the end-plate thickness on the axial load-deformation curves for Type 2 steel column-column connections under axial tension. In the developed FE model, 4 high-strength bolts were arranged close to the column section, the end-plate size is 240×240 mm with thicknesses ranging from 15 mm to 40 mm.

The axial load-deformation curves for the Type 2 connection are depicted in Fig. 16. It can be

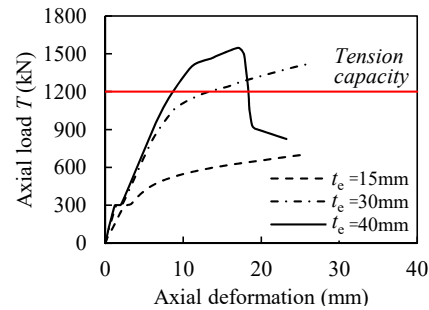


Fig. 16 Effect of end-plate thickness on the load-deformation curves for column connection of Type 2

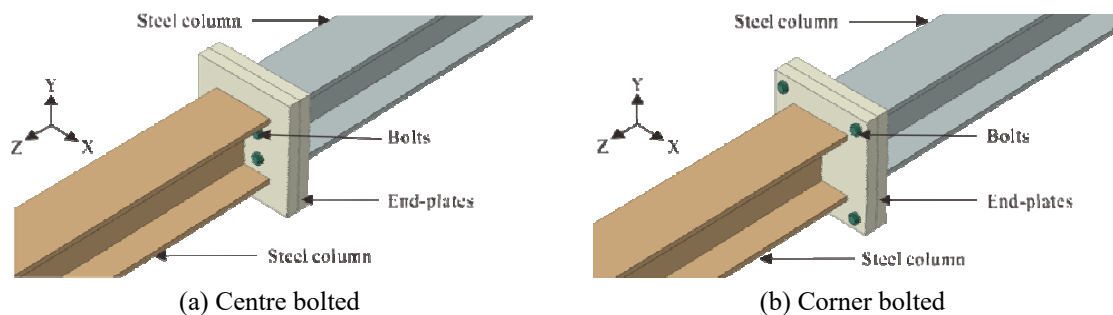


Fig. 17 FE models for connection Type 2 with various bolt positions

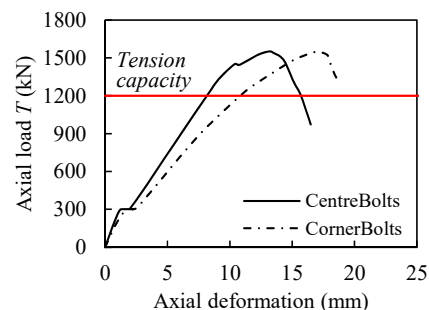


Fig. 18 Effect of the bolt positions on the load-deformation curves for connection Type 2 under axial tension

seen from Fig. 16 that the initial stiffness and ultimate tensile strength increase with increasing the end-plate thickness. The connection with 15 mm and 30 mm thick end-plates fails by end-plates yielding. However, the ultimate tensile strength can be increased by 110% when the end-plate thickness increased from 15 mm to 40 mm, and the connection fails by fracture of bolts, which means the strength of the bolts can be fully used. Moreover, the tensile strength of the connection with 30 mm and 40 mm thick end-plates satisfy the robustness design.

4.2.5 Effect of bolt position

To evaluate the effect of the bolt position on the axial load-deformation curves of steel column-column connections, end-plate with the size of $340 \times 340 \times 40$ mm was utilised in the FE models.

Four high-strength bolts were positioned at the centre and corner respectively, which is shown in Fig. 17. The load-deformation curves are depicted in Fig. 18. It can be observed from Fig. 18 that the ultimate tensile strength and initial stiffness for the centre bolted connection is larger than the connection with corner bolts. However, the corner bolt configuration is generally utilised in the construction industry for easy access and erection.

5. Buckling strength of steel column-column connections

Since column-column connections are part of the column, it must be designed for buckling and stability. Furthermore, concerns about the inaccuracy of the products leading to strength reduction have been raised in the past. To secure the compressive strength of the column-column connection, careful and costly measures like pre-processing of the contact areas of the end section was conducted. In this study, to achieve a better understanding of the axial compressive behaviour of the slender column-column connection and the effect of contact surface imperfection, comparison between FE analysis and design codes was made. The developed FE models are utilised with a column section HE 200B and total length of 4270 mm. The details of each individual model are summarised in Table 4.

In Table 4, λ_x is the slenderness ratio of the column about its major axis, which can be calculated from Eq. (5), while λ_η is the modified member slenderness, which can be calculated by

$$\lambda_\eta = 90 \sqrt{\frac{N_s}{N_{om}}} \quad (7)$$

in which N_s is the nominal section capacity and N_{om} is the elastic flexural buckling load of the member in axial compression (AS4100 1998). In particular, N_s can be calculated by

$$N_s = k_f A_n f_y \quad (8)$$

in which k_f is the form factor, which is the ratio of effective area over the gross area of the section.

In this study, k_f was taken as 1.0. In Eq. (7), N_{om} is the elastic critical buckling force, which can be calculated by

$$N_{om} = \frac{\pi^2 EI}{(k_e L)^2} \quad (9)$$

Table 4 Geometric details of a series of FE models for connection Type 1

L	λ_x	λ_η	$N_{b,rd X}$	$N_{c X}$	N_{FEM}	$N_{FEM Imp}$	N_{FEM}	N_{FEM}	$N_{FEM Imp}$
	EC3	AS4100	EC3	AS4100	Type 1		Type 2	Type 3	
mm	-	-	kN	kN	kN	kN	kN	kN	kN
1500	18	19	2334	2296	2340	2300	2371	2335	2320
3000	35	39	2148	2156	2330	2228	2314	2323	2258
4270	50	55	1959	1966	2235	2146	2290	2285	2200
7000	82	90	1419	1429	1993	1900	2093	2138	1986
10000	117	128	885	893	1700	1570	1788	1847	1631

in which L is the total length of the column-column connection in Table 4. In addition, k_e is the member effective length factor, which was taken as 1.0 due to pin-supports at both ends. N_{c_X} is the nominal member capacities required by AS4100 (1998), which is calculated by

$$N_c = \alpha_c N_s \quad (10)$$

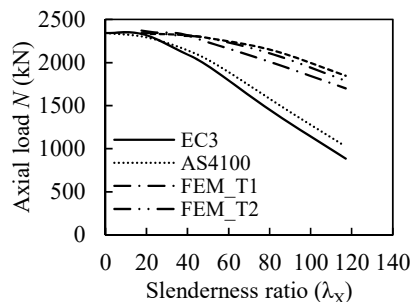
In Table 4, N_{FEM} and $N_{FEM-imp}$ represents the compressive strength of the column-column connection without and with contact surface imperfection along minor axis, respectively.

It can be observed from Fig. 19(a) that the buckling strength required by Eurocode 3 (2005) is more conservative than AS4100 (1998). The buckling strength of connection Type 3 is similar with connection Type 2 and higher than connection Type 1. Figs. 19(b) and (c) present the buckling strength of column-column connections with contact surface imperfection along Y-axis and X-axis, respectively. Due to the existence of welding, initial contact surface imperfection of connection Type 2 is ignored. It is found that the compressive strength of the column-column connection with contact surface imperfection along Y-axis and X-axis is reduced by 10% and 50%, respectively. This is because the contact surface imperfection along the X-axis results in the buckling of column-column connections about its weaker axis, which induces a higher lateral deflection prior to failure. However, even the maximum allowable contact surface imperfection is taken into consideration, the compressive strength of the column-column connection is still sufficient compared with the design codes.

6. Plastic damage in steel column-column connections

The demountability of steel column-column connections depends on the elasticity of both ends of the column sections. The elasticity of the column section is characterised by the ability to exhibit elastic deformation without undergoing significant plastic deformation (Uy *et al.* 2015). The demountability of steel column-column connection cannot be achieved with large plastic deformation occurred in the column sections. The finite element analysis was conducted for predicting the amount of plastic deformation in the column-column connections.

It should be noted that the plastic deformation can be represented by zero equivalent plastic strain (PEEQ). Fig. 20 illustrates large plastic deformation of column sections in various steel column-column connections. It can be seen from Fig. 20 that the large plastic deformation strain



(a) Without contact surface imperfection

Fig. 19 Comparison of buckling strength of various connection types between FE analysis and design codes

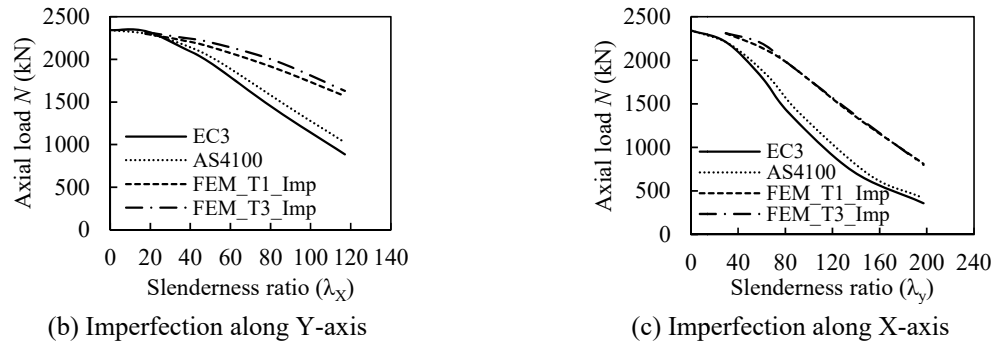


Fig. 19 Continued

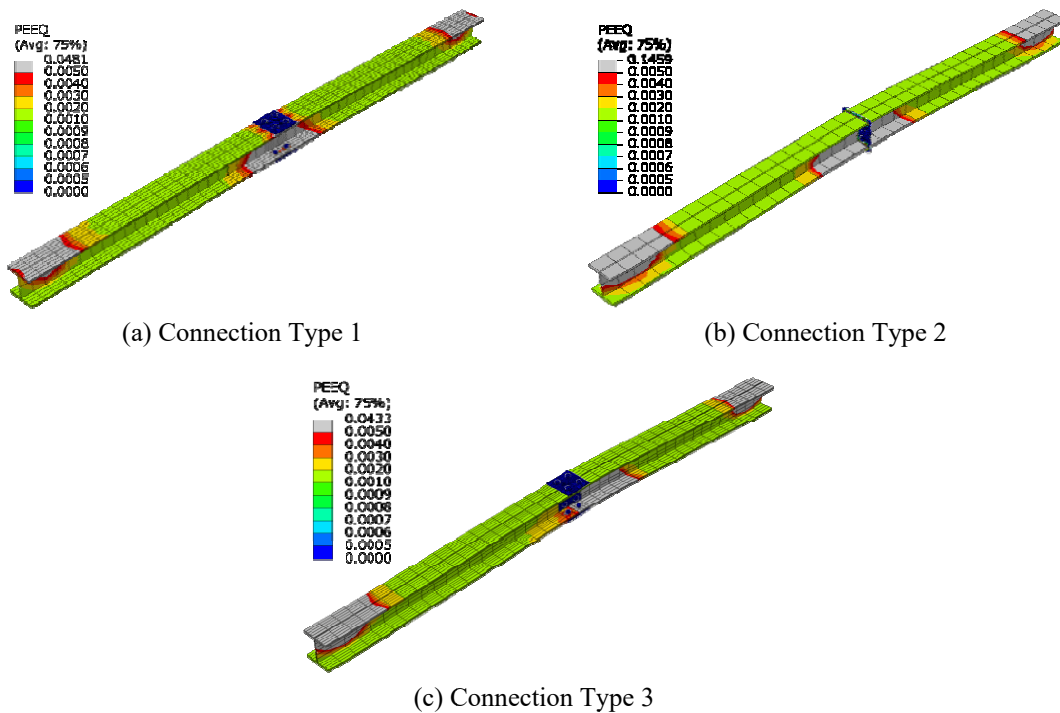


Fig. 20 Large plastic deformation of column section in steel column-column connection

occurred at the regions where the column sections are in contact, as well as the top and bottom ends of the connection, where the restraints are applied.

The applied load-deformation curves for various column-column connections are presented in Fig. 21. It can be observed from Fig. 21 that when the PEEQ is predicted to be less than 0.0015, the column sections for connection Types 1, 2 and 3 can be demounted up to a load of 1465 kN, 1625 kN and 1750 kN, respectively. The loading capacity of these connections to achieve demountability is about 63%, 69% and 75% of their ultimate strength and much greater than the typical service load, which is about 40% of their ultimate strengths. Therefore, when the column-

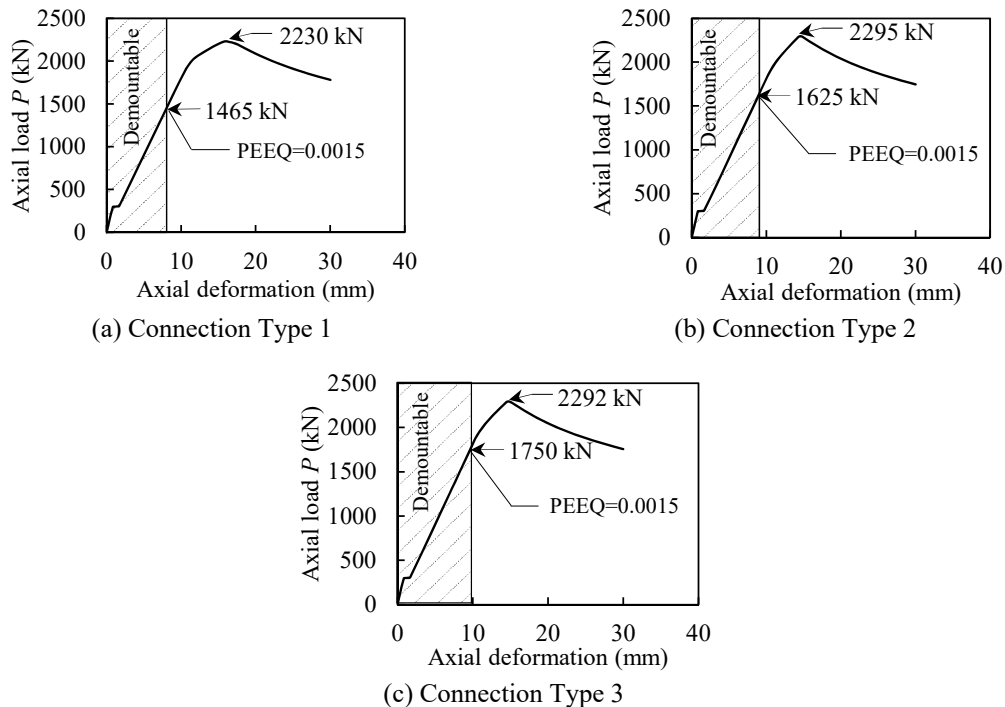


Fig. 21 Applied load-deformation with demountability in column-column connections

column connection is subjected with typical service loads, the column sections can be fully dismantled and reused without additional process or repair.

7. Conclusions

The strength and behaviour of the most commonly used steel column-column connections under axial compression and tension are presented in this paper. The paper innovatively applies the robustness design into steel column-column connections and compares the buckling strength with practical design codes. In addition, the effects of contact surface imperfections on the buckling strength of various connections have been investigated. FE models were developed and validated against experimental results available in the literature and a series of parametric studies were performed. The results obtained from the FE analysis were analysed and the following conclusions can be drawn:

- The increase of slenderness of column-column connections reduces the compressive strength and initial stiffness when the connection is subjected to axial compression. The column-column connection with cover-plates on flanges and web performs higher stiffness than the connection with cover-plates on flanges only.
- The contact surface imperfection along both axes results in a reduction in compressive strength of the connection. Compared with the X-axis inclination, contact surface imperfection along the Y-axis leads to a smaller reduction in compressive strength and initial stiffness. Moreover, when imperfections along both axes exist, the imperfection along the

X-axis governs the load-deformation behaviour of the connection.

- For connections Type 1 and 3 with cover-plates, the thickness of the cover-plate does not have any effect on the load-deformation curves of the column-column connection when subjected to axial compression. However, when the thickness of the cover-plate increases, the tensile strength of the connection increased.
- For connection Type 2 with end-plates, the increase of the end-plate thickness increases the initial stiffness and ultimate strength of the connection. It is found that the thickness of end-plates should be designed large enough, so that the strength of bolts can be fully used and the design tensile strength can be achieved. Furthermore, it is found that the bolts should be designed close to column section to achieve a higher stiffness of the connection.
- Based on the FE analysis, it can be concluded that the steel column-column connection with various connection methods satisfy the buckling requirement from design codes, such as Eurocode 3 (2005) and AS4100 (1998). In particular, the connection with cover-plates on both flanges and web exhibits the better performance over the other two connection methods. Furthermore, the effect of contact surface imperfections on the buckling strength was evaluated and the results indicate that the buckling strength of various connection methods are sufficient even with the maximum allowable imperfection are considered.
- For the steel column-column connections under axial compression, plastic deformation in the contact area of the column-column connection was characterised using equivalent plastic strain (PEEQ). It was found that the column sections of the steel column-column connections with various connection methods can be dismantled whilst the contact region maintains its elasticity without any plastic damage.

Acknowledgments

The research described in this paper is financially supported by the Australian Research Council (ARC) under its Discovery Scheme (Project No: DP140102134). The financial support is gratefully acknowledged.

References

- ABAQUS (2012), Analysis User's Manual; ABAQUS Standard, Version 6.12.
- An, Y.F., Han, L.H. and Zhao, X.L. (2012), "Behaviour and design calculations on very slender thin-walled CFST columns", *Thin-Wall. Struct.*, **53**, 161-175.
- AS1170 (2002), AS1170-2002, Structural design actions; Standards Australia International Ltd.
- AS4100 (1998), AS4100-1998, Steel Structures; Standards Australia International Ltd.
- Gorgolewski, M. (2006), "The implications of reuse and recycling for the design of steel buildings", *Can. J. Civil Eng.*, **33**(4), 489-496.
- Green Building Council of Australia (2009), Green star overview, April. URL: www.gbca.org.au
- Eurocode 1, Part 1-7 (2006), Actions on structures – Accidental actions, European Committee for Standardisation, Brussel, Belgium.
- Eurocode 3, Part 1-8 (2005), Design of steel structures – Design of joints, European Committee for Standardisation, Brussel, Belgium.
- Hanus, F., Zilli, G. and Franssen, J.M. (2011), "Behaviour of Grade 8.8 bolts under natural fire conditions – Tests and model", *J. Constr. Steel Res.*, **67**(8), 1292-1298.
- Hassanein, M.F. and Kharoob, O.F. (2014), "Analysis of circular concrete-filled double skin tubular slender

- columns with external stainless steel tubes”, *Thin-Wall. Struct.*, **79**, 23-37.
- Lee, J., Goldsworthy, H.M. and Gad, E.F. (2010), “Blind bolted T-stub connections to unfiled hollow section columns in low rise structures”, *J. Constr. Steel Res.*, **66**(8-9), 981-992.
- Li, D., Uy, B. and Patel, V.I. (2015), “Behaviour of demountable CFST column-column connections”, *Proceedings of the 2015 International Congress on Advances in Structural Engineering and Mechanics (ASEM15)*, Incheon, Korea, August.
- Lindner, J. (2008), “Old and new solutions for contact splices in columns”, *J. Constr. Steel Res.*, **64**(7-8), 833-844.
- Mago, N. and Hicks, S.J. (2016), “Fire behaviour of slender, highly utilized, eccentrically loaded concrete filled tubular columns”, *J. Constr. Steel Res.*, **119**, 123-132.
- Mirza, O. and Uy, B. (2011), “Behaviour of composite beam-column flush end-plate connections subjected to low-probability, high-consequence loading”, *Eng. Struct.*, **33**(2), 647-662.
- Snijder, B.H.H. and Hoenderkamp, H.J.D. (2008), “Influence of end plate splices on the load carrying capacity of columns”, *J. Constr. Steel Res.*, **64**(7-8), 845-853.
- Swedish Institute of Steel Construction (2005), Sustainability of steel framed buildings, SBI.
- Uy, B. (2014), “Innovative connections for the demountability and rehabilitation of steel”, *Space Composite Structures*, Prague, Czech Republic.
- Uy, B., Patel, V.I. and Li, D. (2015), “Behaviour and design of connections for demountable steel and composite structures”, *Proceedings of the 11th International Conference on Advances in Steel and Concrete Composite Structures*, Beijing, China, December.
- Winters-Downey, E. (2010), “Reclaimed structural steel and LEED Credit MR-3 – Materials Reuse”, *Modern Steel Construction*.